

# Correlation Measurements in $Z \rightarrow \tau^+\tau^-$ and the Leptonic Michel Parameters

## Abstract

Using  $40.3\text{pb}^{-1}$  of data collected with the ALEPH detector at LEP correlations between the decay products of the  $\tau^+$  and  $\tau^-$  produced in the decay of the Z have been measured. The measurements performed in the decays  $\tau \rightarrow e\nu\bar{\nu}$ ,  $\mu\nu\bar{\nu}$ ,  $\pi\nu$ , and  $\rho\nu$  place limits on deviations from the Standard Model. These are given for the leptonic  $\tau$  decays by the parameter set  $\vec{P} = (\rho, \delta, \xi, \eta)$ . The measured values are  $\vec{P} = (0.77 \pm 0.04 \pm 0.04, 0.64 \pm 0.15 \pm 0.07, 1.07 \pm 0.19 \pm 0.20, 0.03 \pm 0.08 \pm 0.07)$ . For models without  $e$ - $\mu$  universality in the charged current interaction the measurements are  $\vec{P}_e = (0.86 \pm 0.07 \pm 0.04, 0.61 \pm 0.40 \pm 0.15, 0.84 \pm 0.30 \pm 0.13, -)$  and  $\vec{P}_\mu = (0.73 \pm 0.05 \pm 0.07, 0.74 \pm 0.27 \pm 0.15, 1.03 \pm 0.30 \pm 0.27, -0.04 \pm 0.09 \pm 0.07)$ . The updated value of the hadronic  $\xi$  parameter and the average  $\tau$ -neutrino helicity is  $\xi = \langle h(\nu_\tau) \rangle = -0.94 \pm 0.05 \pm 0.03$ .

Johannes Raab and Barbara Wolf

Mainz

15. Feb. 1994

## 1 Introduction

This note describes an extension of the correlation measurements [1] to the leptonic sector. In the Standard Model description of  $e^+e^- \rightarrow Z \rightarrow \tau^+\tau^-$  the  $\tau^+$  and  $\tau^-$  are produced with opposite helicities. The Standard Model V-A structure of the charged current leads to a maximal preservation of the original information on the  $\tau$  polarisation in the kinematics of the decay. Thus, deviations from the Standard Model can manifest themselves in the neutral sector by a decrease of the nearly perfect helicity correlation between the  $\tau^+$  and  $\tau^-$  and/or in the charged sector by a different decay distribution in the polarisation sensitive variable.

In the following the results of the investigation of the leptonic  $\tau$  decay spectra are presented. The analysis leads to measurements of the Michel parameters  $\rho$  and  $\xi$ , and of the previously unmeasured parameters  $\delta$  and  $\eta$ . In addition, the enlarged data set relative to [1] is used to update the measurements on the chiral polarisation parameters  $\xi_\tau$ ,  $\xi_\rho$ , and the average  $\tau$ -neutrino helicity.

## 2 Method

In this section the method is briefly reviewed and the extensions to [1] are described. The fundamental equation which describes the decay spectrum in the polarisation sensitive variable,  $z$ , of the  $\tau^\pm$  in the pure helicity state  $h(\tau^\pm)$  is

$$\frac{d\Gamma(\tau^\pm)}{dz} = F(z) \pm h(\tau^\pm) \cdot \xi \cdot G(z). \quad (1)$$

In the hadronic analysis[1]  $F$  and  $G$  are purely kinematic functions. For the leptonic spectra  $F$  and  $G$  depend on the Michel parameters  $\rho$ ,  $\delta$  and  $\eta$  which reflect the Lorentz structure of the charged current interaction [2][3][4]:

$$F(z; \rho, \eta) = 2 - 6z^2 + 4z^3 + \frac{4}{9}\rho(-1 + 9z^2 - 8z^3) + 12\eta\frac{m_\ell}{m_\tau}(1-z)^2 \quad (2)$$

$$G(z; \delta) = -\frac{2}{3} + 4z - 6z^2 + \frac{8}{3}z^3 + \frac{4}{9}\delta(1 - 12z + 27z^2 - 16z^3), \quad (3)$$

where the polarisation sensitive variable  $z$  is defined as  $z = \frac{E_\ell}{E_{beam}}$ , for  $\ell = (e, \mu)$ . *A priori* the Michel parameters  $\vec{\mathcal{P}} = (\rho, \delta, \xi, \eta)$  are not identical for the different leptons.

In the Standard Model the values of the Michel parameters are  $\rho = \frac{3}{4} = \delta$ ,  $\eta = 0$ ,  $\xi = 1$  independent of the lepton family (lepton universality of the charged current). Figure 1 shows the functions  $F$  and  $G$  for several possible parameter combinations. The maximum contribution to  $F$  from the  $\eta$  term – assuming a mixture of V-A and a Higgs-like coupling – is indicated.

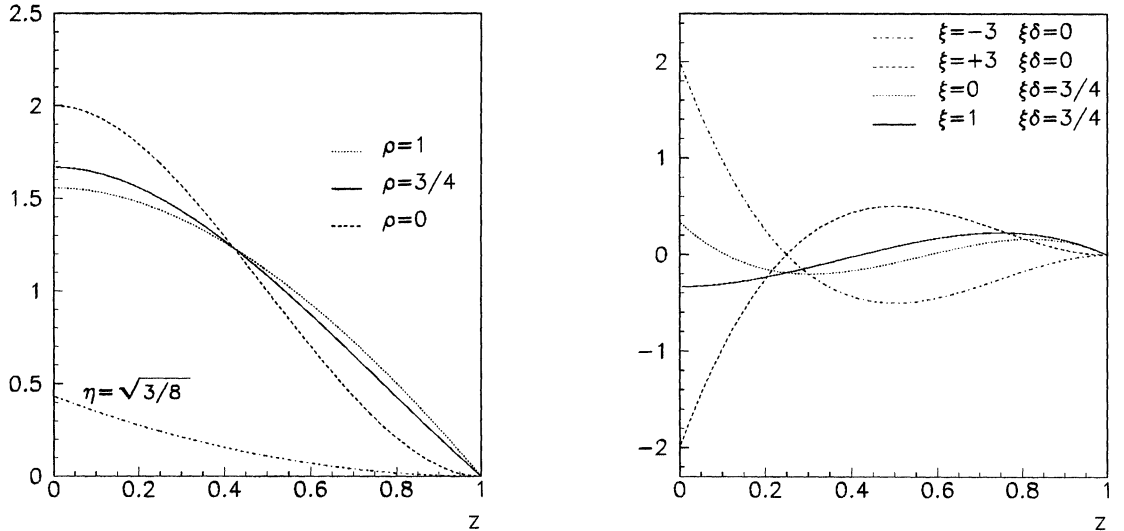


Figure 1: Left: the function  $F$  for three values of  $\rho$  ( $\eta = 0$ ). The maximum contribution to  $F$  from  $\eta$  is also shown. Right: the function  $\xi \cdot G$  for three possible sets of  $(\xi, \delta\xi)$ .

The parameter  $\rho$  is called the *shape* parameter since it has the most influence on the shape of spectrum for unpolarised  $\tau$ . Deviations from lepton universality in the charged current couplings are reflected by  $\delta \neq \frac{3}{4}$ [5]. The parameter  $\xi$  is the *chiral polarisation* parameter but unlike [1] is not directly related to the neutrino helicity. The *spectrum* parameter  $\eta$  is non-zero only when non-standard couplings are present. It is relevant to the prediction of the decay rate or the extraction of the Fermi coupling constant  $G_\tau$ [4][6] since

$$\frac{1}{\tau_\tau} = \frac{m_\tau^5 G_\tau^2}{192\pi^3} \left( 1 + 4\eta \frac{m_\ell}{m_\tau} \right). \quad (4)$$

In  $\tau \rightarrow e\nu\bar{\nu}$  decay  $\eta_e$  is essentially inaccessible but for  $\tau \rightarrow \mu\nu\bar{\nu}$  the sensitivity to  $\eta_\mu$  is comparable to that for  $\rho_\mu$ .

The Michel parameters are bilinear combinations of ten (complex) coupling constants. Their explicit form can be found in [3][4][5][7]. Attention must be paid to differences in notation. From the normalisation condition and the fact that the partial decay widths are always positive, it is possible to derive constraining relationships between the parameters[8][9]:

$$0 \leq \rho \leq 1 \quad (5)$$

$$|\delta \cdot \xi| \leq \rho \quad (6)$$

$$|7\delta \cdot \xi - 3\xi| \leq 9(1 - \rho) \quad (7)$$

The *a priori* allowed region in the  $(\xi, \Delta = \delta\xi)$ -plane is shown in figure 2.

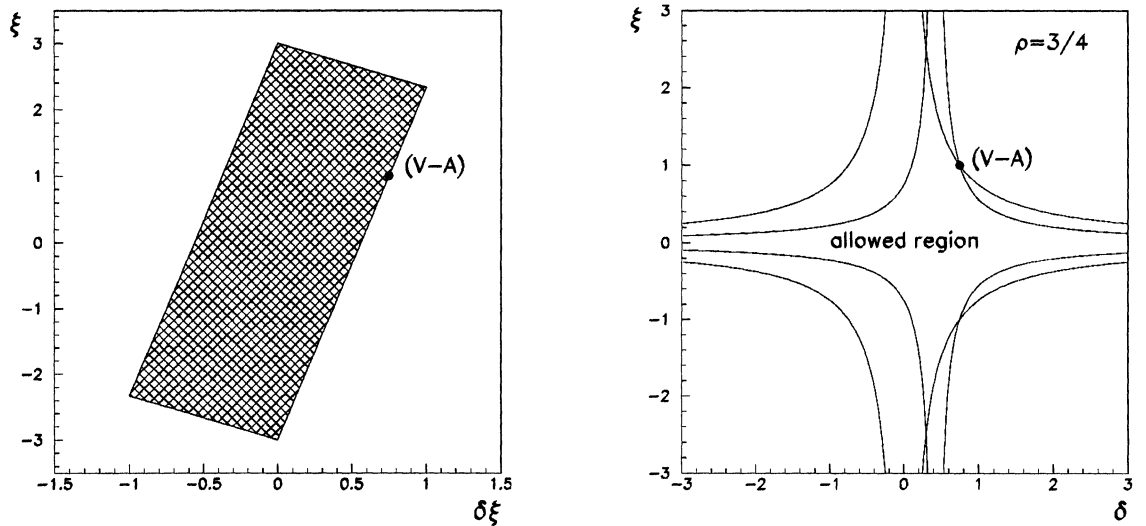


Figure 2: Allowed region in the  $(\xi, \delta\xi)$ -plane (left) and in the  $(\xi, \delta)$ -plane for  $\rho = \frac{3}{4}$  (right).

The correlated spectra for V and A couplings<sup>1</sup> in the neutral current are given by [4][11][12]

$$\frac{d^2\Gamma}{dz_i dz_j} \propto T(z_i, z_j) = F(z_i)F(z_j) + \xi_i \xi_j G(z_i)G(z_j) - p \cdot [\xi_i G(z_i)F(z_j) + \xi_j G(z_j)F(z_i)] \quad (8)$$

where  $p$  is the mean  $\tau^-$  polarisation. The polarisation asymmetry measurement[13] and the  $A_{LR}$  measurement[14] determine the sign of  $p$  unambiguously, so that the eight parameters  $p, \rho_e, \delta_e, \xi_e, \rho_\mu, \delta_\mu, \eta_\mu$  and  $\xi_\mu$  can be completely determined<sup>2</sup>. The uncorrelated spectra (1) provide additional information on the parameters but show a reduced sensitivity and do not determine the relative signs of the  $\xi$ . The sensitivities of the parameters for the leptonic modes are illustrated in figure 3[15].

### 3 Data Analysis

The analysis uses  $40.3pb^{-1}$  of data recorded with the ALEPH detector in the years 1990 to 1992. A detailed description of the detector can be found in [16]. The event selection, the charged particle identification, the decay mode classification, and background rejection are identical to the neural network analysis detailed in [13].

<sup>1</sup>see [10] for a more general case

<sup>2</sup>Ten parameters if  $\xi_\pi$  and  $\xi_\rho$  are included.

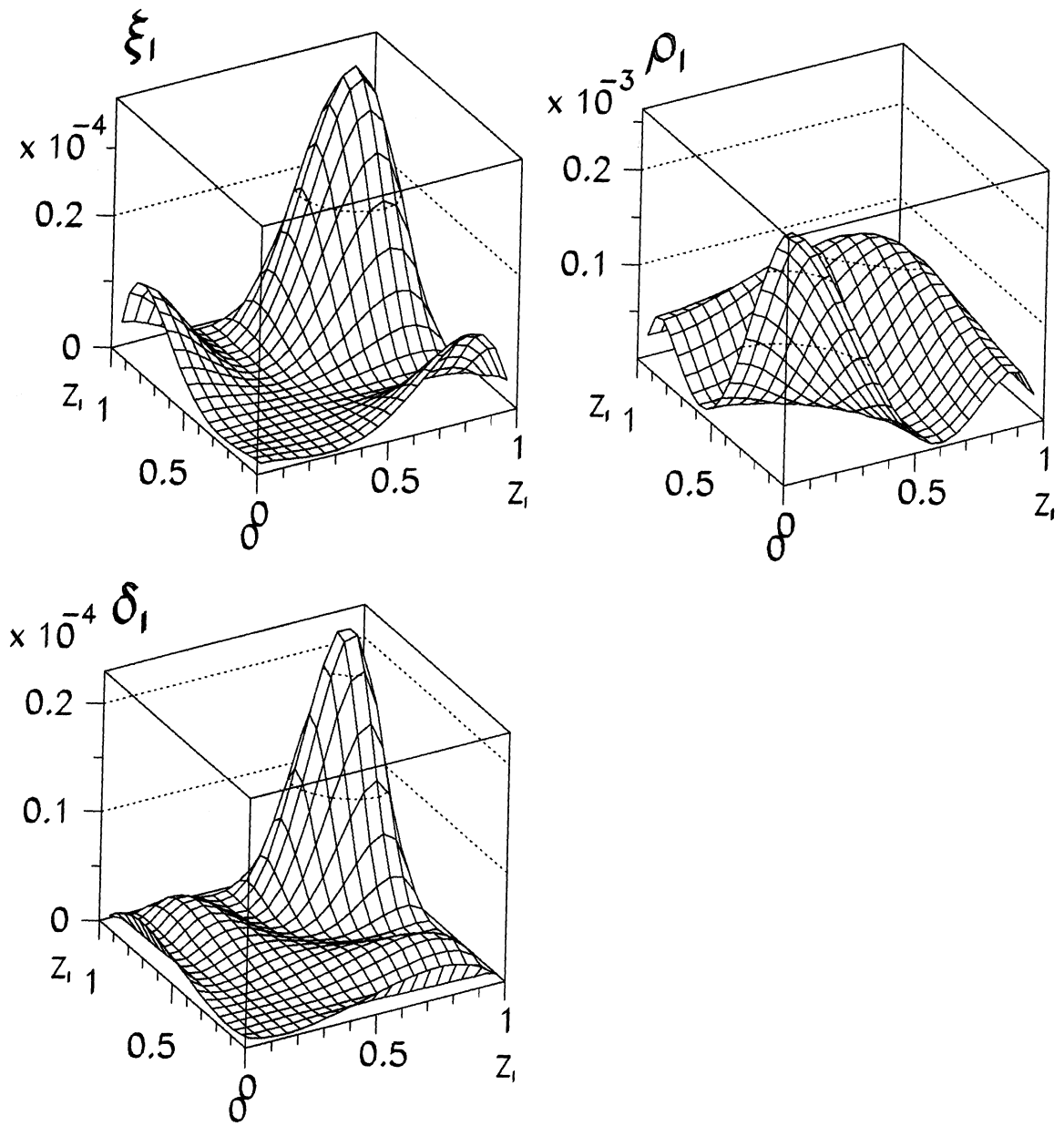


Figure 3: The theoretical sensitivity  $S \equiv \left( \frac{\alpha_i}{\sigma_{\alpha_i}} \right)^2$  for  $ll$ . From top left clockwise  $S(\xi_1)$ ,  $S(\rho)$  and  $S(\delta)$ .

Only  $\tau$  pair candidate events in which at least one of the  $\tau$  decays is classified as  $e$ ,  $\mu$ ,  $\pi$  or  $\rho$  are retained. The events are divided into thirteen exclusive groups consisting of all candidate lepton-lepton, lepton-hadron, hadron-hadron, lepton-X, and hadron-X<sup>3</sup>. The  $ee$  group is excluded due to the large background of radiative Bhabha events. Different from [13] is that the electron momenta are those measured in the TPC – reconstructed soft photons are not added.

The background fractions and the absolute acceptance are extracted from Monte Carlo generated events. The number of reconstructed events, the average acceptance, and the average expected background fraction from  $\tau$  and non- $\tau$  sources are given in table 1.

The data are binned in steps of  $\Delta z = 0.066$  for  $e$ ,  $\mu$ ,  $\rho$  and  $\Delta z = 0.133$  for  $\pi$ . The bin size is smaller than in [1] for better sensitivity (see figure 3). Each year of data gives a set of thirteen histograms. The reason for separating the data sets is twofold: firstly, the different groups show variations in efficiency and background levels from year to year, and secondly, each data set is fit to a different convolution to account for initial and final state radiation (see below). For the years 90 and 91 the efficiencies and background levels are identical within errors so that they are listed in total in table 1.

Since the main thrust of this note concerns the leptonic modes the purely hadronic modes will be neglected unless explicitly stated.

## 4 Measurement of $\vec{\mathcal{P}}$

The spectra of the expected number of events,  $E$ , are fit to the observed distributions  $N$  – the two one-dimensional distributions, and the six two-dimensional distributions – by minimising the negative logarithm of the likelihood function

$$\mathcal{L} = \prod_{i,j,m} \frac{e^{-E(p,\vec{\mathcal{P}};i,j,m)} E(p,\vec{\mathcal{P}};i,j,m)^{N(i,j,m)}}{N(i,j,m)!} \quad (9)$$

with respect to  $p$  and the set of Michel parameters  $\vec{\mathcal{P}}$ . The indices  $i,j$  run over all the bins in the fit range except for the symmetric groups, for which the spectra are folded across the diagonal, so that  $i \geq j$ .

The expected spectra are the sum of the predicted signal events,  $S$ , and the  $\tau$  and non- $\tau$  background,  $B$ :

$$E(p,\vec{\mathcal{P}};i,j,m) = S(p,\vec{\mathcal{P}};i,j,m) + B(i,j,m). \quad (10)$$

The formulae include semi-analytic corrections for initial and final state QED radiation as suggested in [17]<sup>4</sup>. The spectra  $T$  from (1) and (5) are corrected to form  $\hat{T}$  and subsequently folded with resolution and efficiency matrices,  $\mathcal{R}$  and  $\varepsilon$ , determined from simulation. The expected signal distribution is then

$$S(p,\vec{\mathcal{P}};i,j,m) = \sum_{i',j'} \hat{T}(p,\vec{\mathcal{P}};i',j',m) \mathcal{R}(i,i',m) \mathcal{R}(j,j',m) \varepsilon(i,j,m). \quad (11)$$

From equations (1) and (3) it is evident that  $\delta$  and  $\xi$  will be highly correlated through the product  $\xi \cdot \delta$ . In addition, the constraint equations (6) and (7) show that  $\Delta = \xi \cdot \delta$  should be considered as an independent variable. For these reasons the fit treats  $(\Delta, \xi)$  as independent variables rather than  $(\delta, \xi)$ .

<sup>3</sup>The two groups  $\pi X$  and  $\rho X$  are not identical with those used in [1]. In [1]  $(e, \mu)\pi^-$  and  $(e, \mu)\rho^-$  candidates fall into the categories  $\pi X$  and  $\rho X$ .

<sup>4</sup>The radiative corrections for the  $\eta$ -term are given by

$$\eta(1-x)^2 \rightarrow \eta \left[ (1-x)^2 + (1-x)^2 \ln(1-x) - \left( \frac{1}{2} - x + x^2 \right) \ln x - \frac{1}{2}(1-x) \right].$$

data set	group	# of events reconstructed	$\langle \epsilon \rangle$ [%]	estimated background [%]	
				$\tau$	non- $\tau$
90+91	$e\mu$	924	$69.1 \pm 0.4$	$3.3 \pm 0.2$	$0.8 \pm 0.3$
	$e\pi$	434	$40.3 \pm 0.5$	$9.3 \pm 0.5$	$0.6 \pm 0.4$
	$e\rho$	638	$34.1 \pm 0.4$	$7.4 \pm 0.3$	$0.3 \pm 0.2$
	$\mu\mu$	481	$60.8 \pm 0.6$	$2.6 \pm 0.2$	$2.2 \pm 0.7$
	$\mu\pi$	545	$54.1 \pm 0.6$	$7.6 \pm 0.4$	$0.5 \pm 0.3$
	$\mu\rho$	852	$41.5 \pm 0.4$	$7.1 \pm 0.3$	$0.1 \pm 0.1$
	$\pi\pi$	168	$46.4 \pm 0.9$	$11.7 \pm 0.9$	$0.6 \pm 1.0$
	$\pi\rho$	499	$36.8 \pm 0.5$	$12.4 \pm 0.5$	$0.1 \pm 0.2$
	$\rho\rho$	438	$29.1 \pm 0.5$	$12.3 \pm 0.6$	$0.5 \pm 0.6$
	$eX$	1784	$73.3 \pm 0.4$	$2.1 \pm 0.1$	$2.2 \pm 0.3$
	$\mu X$	2209	$98.2 \pm 0.1$	$1.4 \pm 0.1$	$1.9 \pm 0.3$
	$\pi X$	1642	$97.4 \pm 0.1$	$7.8 \pm 0.1$	$3.1 \pm 0.4$
	$\rho X$	2367	$69.1 \pm 0.4$	$6.5 \pm 0.2$	$1.0 \pm 0.2$
	92	$e\mu$	1400	$67.1 \pm 0.4$	$3.4 \pm 0.2$
$e\pi$		590	$38.1 \pm 0.5$	$10.2 \pm 0.5$	$0.1 \pm 0.1$
$e\rho$		1080	$32.9 \pm 0.4$	$9.2 \pm 0.4$	$0.1 \pm 0.1$
$\mu\mu$		696	$57.8 \pm 0.6$	$1.8 \pm 0.2$	$7.2 \pm 1.1$
$\mu\pi$		763	$51.8 \pm 0.6$	$9.1 \pm 0.4$	$0.1 \pm 0.1$
$\mu\rho$		1219	$40.3 \pm 0.4$	$7.9 \pm 0.3$	$0.1 \pm 0.1$
$\pi\pi$		248	$44.4 \pm 1.0$	$16.5 \pm 1.1$	$0.1 \pm 0.1$
$\pi\rho$		731	$35.5 \pm 0.5$	$15.6 \pm 0.6$	$0.1 \pm 0.1$
$\rho\rho$		623	$29.1 \pm 0.4$	$14.1 \pm 0.6$	$0.1 \pm 0.1$
$eX$		2650	$76.5 \pm 0.3$	$2.7 \pm 0.1$	$0.1 \pm 0.1$
$\mu X$		3532	$99.1 \pm 0.1$	$1.3 \pm 0.1$	$2.9 \pm 0.3$
$\pi X$		2460	$98.8 \pm 0.1$	$8.6 \pm 0.2$	$1.8 \pm 0.3$
$\rho X$		3923	$75.0 \pm 0.3$	$7.3 \pm 0.2$	$0.1 \pm 0.1$

Table 1: Number of reconstructed events, the average efficiency  $\langle \epsilon \rangle$ , and the expected background from  $\tau$  and non- $\tau$  sources for each event group and data set.

The constraints are realised through a redefinition of the fit parameters, for example  $\Delta \rightarrow \rho \cdot \tanh(x)$ . After convergence, the parameters and their errors are transformed back into the standard basis.

On account of the complexity of the fit it is natural to inquire how well the method reproduces the Standard Model input values of the Monte Carlo simulations. To this end, the resolution and efficiency matrices from one set of simulations are used as input to fit to another set of simulations. Table 2 gives a comparison between the input and fitted parameters. No significant shortcomings of the method are observed. Nevertheless, these deviations are included as systematic uncertainties due to the method itself in table 5.

parameter	input	fit result
$p$	-0.130	$-0.145 \pm 0.009$
$\rho_e$	0.75	$0.71 \pm 0.06$
$\delta_e$	0.75	$0.74 \pm 0.02$
$\xi_e$	1.0	$1.14 \pm 0.11$
$\rho_\mu$	0.75	$0.72 \pm 0.01$
$\delta_\mu$	0.75	$0.71 \pm 0.06$
$\xi_\mu$	1.0	$1.12 \pm 0.10$
$\eta_\mu$	0.0	$-0.01 \pm 0.03$

Table 2: Michel Parameters obtained from a fit to  $\tau$  pair Monte Carlo events at generator level.

The fit results for various constraints are given in table 3 and shown in figure 4. The numbers in column (a) are obtained by assuming universality of the charged current. For column (b) the constraints are added. Column (c) contains results without the universality assumption and no constraints. Table 4 list the correlation coefficients for fits (a) and (c).

parameter	fit type		
	(a)	(b)	(c)
$p$	$-0.198 \pm 0.033$	$-0.198 \pm 0.033$	$-0.199 \pm 0.035$
$\rho_e$	$0.77 \pm 0.04$	$0.77 \pm 0.04$	$0.86 \pm 0.07$
$\delta_e$	$0.64 \pm 0.16$	$0.64 \pm 0.14$	$0.61 \pm 0.42$
$\xi_e$	$1.07 \pm 0.19$	$1.07 \pm 0.19$	$0.84 \pm 0.31$
$\rho_\mu$	—	—	$0.73 \pm 0.05$
$\delta_\mu$	—	—	$0.74 \pm 0.33$
$\xi_\mu$	—	—	$1.03 \pm 0.38$
$\eta_\mu$	$0.03 \pm 0.08$	$0.03 \pm 0.08$	$-0.04 \pm 0.09$
$\chi^2$	3541	3541	3538
$N_{dof}$	3796	3796	3793

Table 3: Fit results for the following constraints: (a) universality, no bounds, (b) universality, with bounds, (c) no universality, no bounds.

The influence of the boundary conditions on the absolute values of the errors are minor. Insofar as the best fit parameter set is at the boundary curve, only the one-sided errors are relevant. This is illustrated in figures 4 which are contour level diagrams of  $\ln \mathcal{L}$  in the  $\Delta\xi$  and  $\delta\xi$  plane with and without constraints.

## 5 Systematic Uncertainties

The primary sources of systematic errors have been discussed previously in [1][13]. The various contributions are summarised in table 5.

correlation coefficients									
fit	parameter	$p$	$\Delta$	$\rho$	$\xi$	$\eta$			
(a)	$p$	1	-0.07	0.34	0.14	0.04			
	$\Delta$		1	0.35	0.06	-0.12			
	$\rho$			1	-0.21	0.35			
	$\xi$				1	0.22			
	$\eta$					1			
(c)	parameter	$p$	$\Delta_e$	$\rho_e$	$\xi_e$	$\Delta_\mu$	$\rho_\mu$	$\xi_\mu$	$\eta_\mu$
	$p$	1	-0.12	0.35	-0.04	-0.08	0.56	0.42	0.29
	$\Delta_e$		1	-0.64	0.48	0.05	-0.03	0.00	0.02
	$\rho_e$			1	-0.64	0.06	0.15	0.12	0.05
	$\xi_e$				1	-0.10	0.04	-0.04	0.02
	$\Delta_\mu$					1	-0.39	-0.05	-0.18
	$\rho_\mu$						1	0.21	0.55
	$\xi_\mu$							1	0.59
	$\eta_\mu$								1

Table 4: Correlation coefficients for fit type (a) and (c).

source	$\Delta p$	$\Delta \rho$	$\Delta \delta$	$\Delta \xi$	$\Delta \eta$				
Monte Carlo statistics	0.011	0.01	0.05	0.06	0.03				
background ( $\pm 30\%$ )	0.017	0.01	0.01	0.02	0.04				
correlated background cuts	0.025	0.03	0.03	0.16	0.03				
efficiency	0.021	0.02	0.01	0.01	0.01				
correlated efficiency	0.024	0.02	0.04	0.09	0.03				
uncertainties in method	0.006	0.01	0.01	0.05	0.01				
sum in quadrature	0.045	0.04	0.07	0.20	0.07				
	$\Delta p$	$\Delta \rho_e$	$\Delta \delta_e$	$\Delta \xi_e$	$\Delta \rho_\mu$	$\Delta \delta_\mu$	$\Delta \xi_\mu$	$\Delta \eta_\mu$	
Monte Carlo statistics	0.012	0.02	0.14	0.10	0.02	0.11	0.13	0.03	
background ( $\pm 30\%$ )	0.014	0.01	0.01	0.01	0.01	0.01	0.01	0.02	
correlated background cuts	0.031	0.01	0.01	0.06	0.03	0.01	0.23	0.04	
efficiency	0.013	0.01	0.01	0.01	0.01	0.01	0.01	0.02	
correlated efficiency	0.024	0.03	0.04	0.04	0.05	0.10	0.04	0.03	
uncertainties in method	0.006	0.01	0.01	0.03	0.02	0.01	0.02	0.01	
sum in quadrature	0.045	0.04	0.15	0.13	0.07	0.15	0.27	0.07	

Table 5: Systematic uncertainties in the Michel parameters.



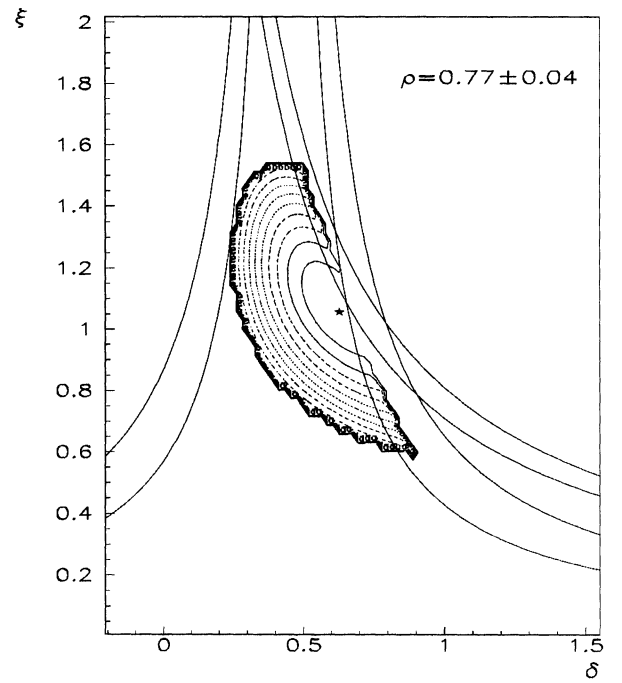
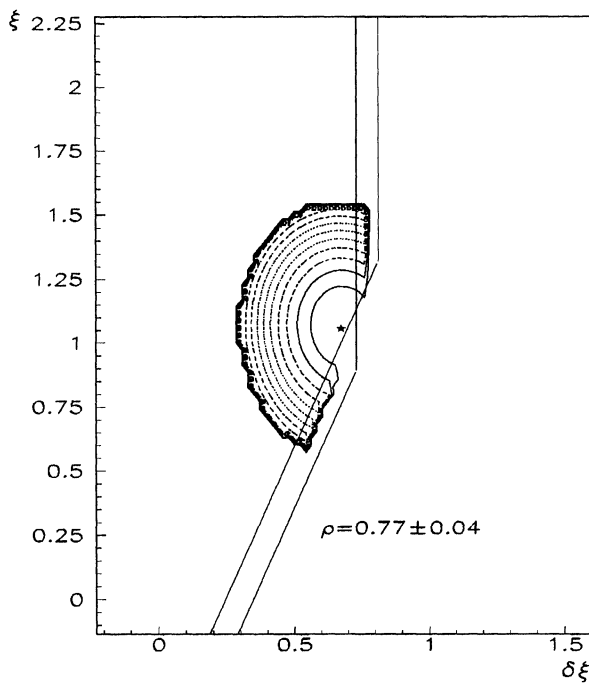
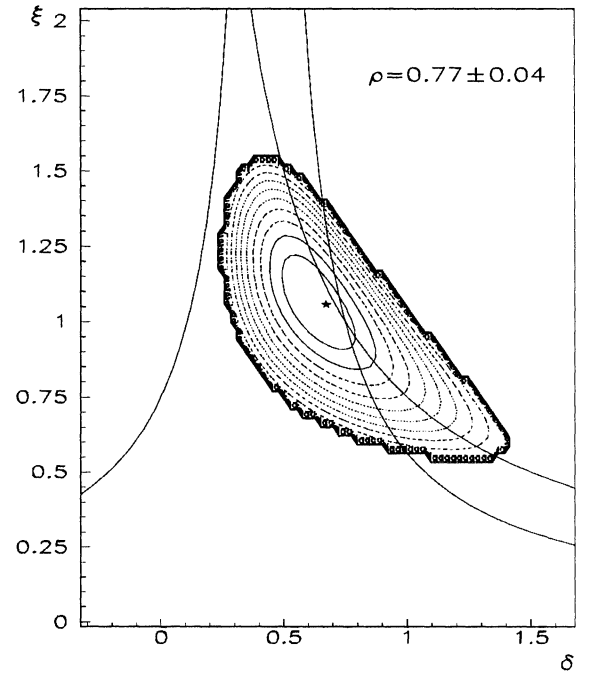
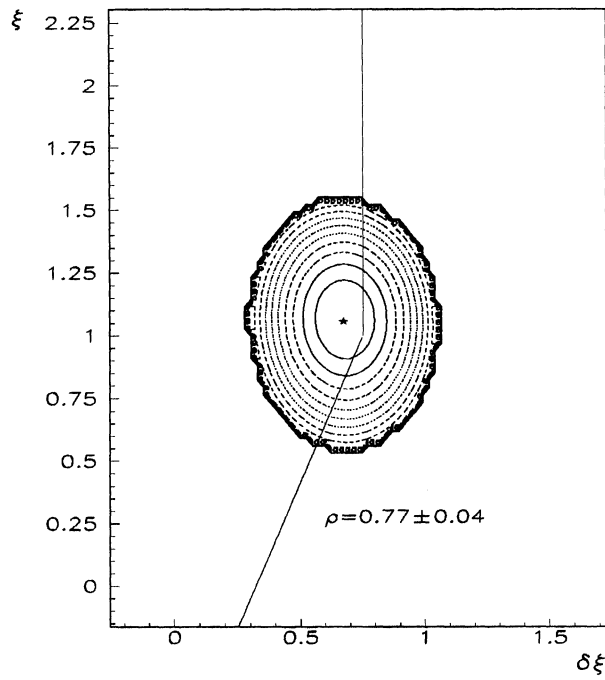


Figure 4: Contour levels in steps of  $1\sigma$  in  $(\xi, \Delta)$ -plane (left) and in  $(\xi, \delta)$ -plane (right) for fit (a) (top). Contour levels for fit (b) (bottom).

Since the spectra are non-linear in the kinematic variable  $z$  the *slope* corrections include non-linear terms to examine possible deviations from linearity between Monte Carlo and data [18][19]. The *slope* parameters and their statistical uncertainties are given in table 6. The influence of these uncertainties are included in table 5 under the heading *correlated efficiency*.

	$a$	$b$	$c$	$d$
$e$	$1.007 \pm 0.002$	$0.001 \pm 0.005$		
	$1.012 \pm 0.004$	$-0.001 \pm 0.005$	$0.060 \pm 0.045$	
	$1.000 \pm 0.008$	$-0.026 \pm 0.020$	$0.040 \pm 0.043$	$0.13 \pm 0.11$
$\mu$	$0.995 \pm 0.002$	$0.009 \pm 0.004$		
	$1.005 \pm 0.004$	$0.020 \pm 0.008$	$-0.051 \pm 0.031$	
	$1.003 \pm 0.003$	$0.042 \pm 0.010$	$-0.033 \pm 0.032$	$0.16 \pm 0.08$

Table 6: Parametrisation of  $\frac{\varepsilon_{data}}{\varepsilon_{mc}} = a + bx + cx^2 + dx^3$  for the 1991 data set.

Following the method and selection given in [1], the values for the hadronic chiral polarisation parameters are  $\xi_\pi = -0.95 \pm 0.08 \pm 0.04$ ,  $\xi_\rho = -0.93 \pm 0.08 \pm 0.04$ , and  $\xi = -0.94 \pm 0.05 \pm 0.03$ . These measurements are completely independent of the leptonic analysis.

## 6 Conclusions

Within the framework of V and A type couplings in the production of  $\tau$  pairs at the Z resonance the Michel parameters in the decays  $\tau \rightarrow e(\mu)\nu\bar{\nu}$  have been measured. For the first time the parameters  $\delta$  and  $\eta$  have been measured directly in  $\tau$  decays.

$$\begin{aligned}
 \rho &= 0.77 \pm 0.04 \pm 0.04 \\
 \delta &= 0.64 \pm 0.15 \pm 0.07 \\
 \xi &= 1.07 \pm 0.19 \pm 0.20 \\
 \eta &= 0.03 \pm 0.08 \pm 0.07
 \end{aligned}$$

Assuming that the charged current interaction does not obey the universality condition, then the following measurements hold:

$$\begin{aligned}
 \rho_e &= 0.86 \pm 0.07 \pm 0.04 & \rho_\mu &= 0.73 \pm 0.05 \pm 0.07 \\
 \delta_e &= 0.61 \pm 0.40 \pm 0.15 & \delta_\mu &= 0.74 \pm 0.27 \pm 0.15 \\
 \xi_e &= 0.84 \pm 0.30 \pm 0.13 & \xi_\mu &= 1.03 \pm 0.30 \pm 0.27 \\
 & & \eta_\mu &= -0.04 \pm 0.09 \pm 0.07.
 \end{aligned}$$

Finally, the updated value of the average  $\tau$  neutrino helicity is

$$\langle h(\nu_\tau) \rangle = \xi = -0.94 \pm 0.05 \pm 0.03. \quad (12)$$

The measurement of  $\eta$  compares very well to the value extracted from the ratio of leptonic widths[22]:

$$\eta = \frac{m_\tau}{4m_\mu} \left( \frac{\Gamma(\tau \rightarrow e\nu\bar{\nu})}{\Gamma(\tau \rightarrow \mu\nu\bar{\nu})} - 1 \right) = 0.08 \pm 0.09.$$

The measurements of  $\rho$  and  $|\xi|$  are in good agreement with those obtained by ARGUS  $\rho = 0.742 \pm 0.035 \pm 0.020$ ,  $|\xi| = 0.90 \pm 0.15 \pm 0.10$ ,  $\rho_e = 0.747 \pm 0.045 \pm 0.028$ ,  $\rho_\mu = 0.734 \pm 0.055 \pm 0.027$ ,  $\rho = 0.742 \pm 0.035 \pm 0.020$  [21], and  $\xi_{a_1} = -1.25 \pm 0.23_{-0.08}^{+0.15}$  [20].

None of these measurements shows disagreement with Standard Model expectation at the current level of precision. With additional data from 1993-1995 and an improved understanding of the systematic uncertainties, especially in the background rejection and the efficiency correlation, ALEPH can make a significant contribution to measurements of the charged current.

**Note added:** The quoted systematic errors are very conservative due to a disagreement between the EP and UW analysis in the electron channel. These disagreements are now resolved and work is in progress to adjust the errors correspondingly.

## References

- [1] ALEPH Collab., *Correlation Measurements in  $Z \rightarrow \tau^+\tau^-$  and the  $\tau$  Neutrino Helicity*, CERN-PPE 93-181, submitted to Phys. Lett. B.
- [2] L. Michel, Proc. Phys. Soc. A63, (1959), 514.
- [3] F. Scheck, Phys. Rep. 44, (1978), 187.
- [4] W. Fetscher, Phys. Rev. D42, (1991), 1544.
- [5] K. Mursula and F. Scheck, Nucl. Phys. B253, (1985), 189.
- [6] K. Mursula, M. Roos, and F. Scheck, Nucl. Phys. B219, (1983), 321.
- [7] G. Hughes et al., *A Measurement of the Michel Parameters in Leptonic Tau Decays*, ALEPH 92-104.
- [8] T. Kinoshita and A. Sirlin, Phys. Rev. 108, (1957), 844.
- [9] N. Kemmer, Univ. of Lancaster, internal report, (1993).
- [10] U. Stiegler, Z. Phys. C58, (1993), 601.
- [11] S.-Y. Pi and A. I. Sanda, Ann. of Phys. 106, (1977), 171.
- [12] C. Nelson, Phys. Rev. D40, (1989), 123; *Erratum*: Phys. Rev. D41, (1990), 2327.
- [13] ALEPH Collab., Z. Phys. C59, (1993), 369.
- [14] SLD Collab., Phys. Rev. Lett. 70, (1993), 2515.
- [15] B. Wolf, *Measurement of Michel Parameters and  $\tau$  Neutrino Helicity in  $Z \rightarrow \tau^+\tau^-$* , Ph.D. thesis, Johannes-Gutenberg-Universität Mainz, (1994).
- [16] ALEPH Collab., Nucl. Instr. Meth. A294, (1990), 211.
- [17] S. Jadach and Z. Was, *Z Physics at LEP I*, CERN 89-08, eds. G. Altarelli, *et. al.*.
- [18] J. Conway, J. Harton, M. Schmitt, and M. Walsh, *Tau and Electron Couplings to the Z from Measurement of the Tau Polarization in ALEPH*, ALEPH 92-77.
- [19] J. Harton and M. Walsh, *Performance of Neural Net Particle Identification in 1992*, ALEPH 93-189.
- [20] ARGUS Collab., Z. Phys. C58, (1993), 61.
- [21] ARGUS Collab., Phys. Lett. B246, (1990), 278; Phys. Lett. B316, (1993), 608.
- [22] PDG, Phys. Rev. D45, (1992).